

# Optimized cluster theory, the Lennard-Jones fluid, and the liquid-gas phase transition\*

Stephen H. Sung

*Department of Physics, University of Illinois, Urbana, Illinois 61801*

David Chandler<sup>†</sup>

*School of Chemical Sciences, University of Illinois, Urbana, Illinois 61801*

(Received 12 October 1973)

The optimized cluster theory is applied to the Lennard-Jones fluid. The coexistence curve obtained from the theory is presented. It represents the most accurate microscopic calculation of the liquid-gas phase diagram for a fluid with a realistic Hamiltonian. The theory is shown to be quantitatively accurate for all fluid states except those very close to the critical point. Phenomenological procedures are devised which extrapolate towards the critical point from regions in which the optimized cluster theory is accurate. The extrapolation calculations predict nonclassical values for the critical exponents which are in fairly good agreement with experiment. In addition to investigating the liquid-gas phase transition, the equilibrium pair correlation functions are calculated at several states. Further, the internal consistency of the optimized cluster theory is discussed.

## I. INTRODUCTION

Much progress has been made recently in the theory of simple liquids.<sup>1</sup> The principal physical concept associated with this progress originated with the work of van der Waals. This is the idea that for a dense fluid, the repulsive forces (which are nearly hard-sphere interactions) dominate the intermolecular structure. Indeed, it has been shown<sup>1-4</sup> that the radial distribution function  $g(r)$  for a dense Lennard-Jones (LJ) liquid agrees closely with that for the fluid in which the interactions are just the LJ repulsions and there are no attractive forces.

A qualitative explanation of this structural phenomenon follows from a simple description of the environment of a particle in a dense liquid. For the LJ fluid, high density corresponds to thermodynamic states at which  $\rho^{-1/3} \lesssim r_0$ , where  $\rho$  is the particle density and  $r_0$  is the location of the minimum in the LJ potential. (A glance at a phase diagram shows that "high density" characterizes most of the liquid phase outside the critical region; see Fig. 2 in Sec. III of this paper.) Because  $\rho^{-1/3} \lesssim r_0$ , nearest neighbors in a dense liquid are crushed extremely close to one another, and any displacement of a particle will cause a large change in the energy associated with the interparticle repulsive forces. However, the change in energy associated with the attractive forces will be relatively small because these interactions are not quickly varying functions of the interparticle separation. As a result, the repulsions dominate the high-density structure.

At low and moderate densities, particles are

not so close together, and the longer-ranged attractive forces can play a significant role in forming the structure. Indeed, in the extreme limit of zero density, the effects on  $g(r)$  due to repulsions and due to attractions are comparable in size.

Thus, the relative importance of the attractive forces on the interparticle correlations in a fluid becomes smaller as the density is increased. The mechanism for this reduction is "repulsive force screening": the particles are so close to one another at high densities that the repulsive forces form a structure (essentially due to excluded volume effects) which is not appreciably changed by the attractive interactions.<sup>5</sup>

The optimized cluster theory (OCT) introduced by Andersen and Chandler<sup>6,7</sup> provides a microscopic theory for the structural phenomenon described above. The purpose of this paper is to present the predictions of this theory when it is applied to the LJ fluid in the vicinity of the liquid-gas phase transition. We will show in Sec. III that the OCT is quantitatively accurate except for thermodynamic states very close to the critical point.

The principal procedure in the OCT is a rearrangement of the Mayer cluster expansion which allows one to replace the attractive interactions with an "optimized" renormalized potential. This renormalized (or screened) potential embodies the repulsive force screening which reduces the effect of the attractions at high densities. At low densities, the repulsive force screening does not exist, and the OCT renormalized potential becomes, in the limit of zero density, the bare at-

tractive interaction.

In Sec. II, the OCT is reviewed; the precise definition of the optimized renormalized potential is given; and the internal consistency of the OCT is examined. Then, in Sec. III, the theory is applied to study the LJ fluid for thermodynamic states of low, moderate, and high densities. The liquid-gas phase diagram is calculated, and the theory is used to study correlation functions and thermodynamic properties near the critical point. The paper is concluded with a discussion in Sec. IV.

This paper has been written with the assumption that the reader is familiar with recent publications on the theory of simple liquids. The particular papers that we regard as prerequisites to the present paper are Refs. 3, 4, and 6. The notation and terminology which we use are consistent with the notation and terminology used in those references.

## II. THEORY

### A. Review of optimized cluster theory

As presented in Ref. 6, the OCT is applicable to a system in which the total potential energy is a sum of pair interactions, and the pair potential is of the form  $w(r) = u_d(r) + u(r)$ , where  $u_d(r)$  is the hard-sphere potential, i.e.,

$$\begin{aligned} u_d(r) &= \infty, \quad r \leq d \\ &= 0, \quad r > d. \end{aligned}$$

The fluid composed of hard spheres of diameter  $d$  is the reference (or unperturbed) system, and  $u(r)$  is the perturbation.

Rather than expand properties of the total system in a perturbation series that is ordered in powers of  $u(r)/k_B T$  ( $k_B$  is Boltzmann's constant and  $T$  is the temperature), the OCT uses a rearrangement of this series to express the effects of the perturbation in terms of a renormalized potential. The renormalized interaction is  $-k_B T \mathcal{C}(r)$ , where  $\mathcal{C}(r)$  is the sum of simple chains of cluster diagrams involving  $-u(r)/k_B T$  bonds and reference system pair correlation function bonds. The mathematical formula for  $\mathcal{C}(r)$  is given by Eq. (3.8) of Ref. 6.

The incorporation of repulsive force screening is made with the "optimization condition" which is defined mathematically by Eqs. (4.1) and (4.1') of Ref. 6. It is important that the formulas written below are used together with the optimization condition. If the optimization is not performed, the formulas will not include the physics of repulsive force screening; and without this physics, the formulas are not accurate.

A discussion of how the optimization procedure incorporates repulsive force screening into the OCT is given in Ref. 6. In addition to that discussion, it can be shown<sup>8</sup> that the optimization procedure inserts into the renormalized potential an infinite class of (topologically specifiable) diagrams that are not contained in the unoptimized renormalization.

With  $-k_B T \mathcal{C}(r)$  denoting the optimized renormalized potential, the principal results of the OCT are

$$g(r) \approx g_{\text{EXP}}(r) = g_d(r) \exp[\mathcal{C}(r)] \quad (2.1)$$

and

$$\mathcal{Q} \approx \mathcal{Q}_{\text{ORPA} + B_2} = \mathcal{Q}_{\text{HTA}} + a_{\text{RING}} + B_2. \quad (2.2)$$

Here, we use the notation and terminology established in Ref. 6:  $g_d(r)$  is the radial distribution function for the hard-sphere fluid;  $\mathcal{Q}$  is the Helmholtz free-energy density; and  $\mathcal{Q}_{\text{HTA}}$  is the free-energy density which gives the exact  $\mathcal{Q}$  through first order in  $u(r)/k_B T$  [it is the result obtained for  $\mathcal{Q}$  if one assumes that the perturbation does not affect the structure, i.e.,  $g(r) \approx g_d(r)$ ].<sup>3,4</sup> The sum  $\mathcal{Q}_{\text{HTA}} + a_{\text{RING}}$  is the optimized-random-phase approximation (ORPA) for  $\mathcal{Q}$ .<sup>4</sup> The quantity  $B_2$  is like a second virial coefficient; however, it involves the renormalized perturbation rather than the bare interaction  $u(r)$ .<sup>6</sup>

The evaluation of Eqs. (2.1) and (2.2) requires the knowledge of the free-energy and pair correlation function for the hard-sphere fluid. This information is obtained from the Verlet-Weis formula for  $g_d(r)$ <sup>9</sup> and the Carnahan-Starling formula for the equation of state.<sup>10</sup> These equations summarize in analytic form the results of exact machine calculations on the hard-sphere system.

Equations (2.1) and (2.2) are exact in the low-density limit.<sup>6</sup> Furthermore, because the repulsive force screening is described by the optimized  $\mathcal{C}(r)$ , these equations are extremely accurate at high densities.<sup>7</sup> At moderate densities, however, it is not obvious that they will remain quantitatively precise. It is the moderate density region in which the liquid-gas phase transition occurs. For this reason, the results reported in Sec. III are concerned mainly with thermodynamic states in the vicinity of the liquid-gas coexistence curve.

The corrections to the approximations given in Eqs. (2.1) and (2.2) are written explicitly in Ref. 6 as infinite series involving  $g_d(r)$  and  $\mathcal{C}(r)$ . The expansion parameter in the series is  $\lambda \approx \rho R^3 \bar{\mathcal{C}}$ . Here,  $R$  denotes the range of the renormalized potential, and  $\bar{\mathcal{C}}$  is the average magnitude of the renormalized potential. Except for states near a critical point,  $R$  is of the order of the particle diameter  $d$ .

If necessary, it is always possible to use higher-order terms in the optimized cluster expansions and evaluate corrections to Eqs. (2.1) and (2.2). However, if  $\lambda$  is small, this is not necessary since it is shown in Ref. 6 that for each value of  $r$  the fractional error in  $g(r) \approx g_{\text{EXP}}(r)$  (which is called the exponential approximation) is of order  $\lambda$ , and the error in  $\mathcal{G} \approx \mathcal{G}_{\text{ORPA+B}_2}$  is of order  $\lambda^2$ . For the fluid studied in this paper  $\rho d^3 \bar{c} \sim 10^{-2}$  for all fluid states. As a result, except for points in the critical region [where  $(R/d)^3$  becomes relatively large],  $\lambda$  is small enough that the corrections to Eqs. (2.1) and (2.2) are negligible.

The theory which we summarily call the OCT is the EXP (exponential) approximation for  $g(r)$ , Eq. (2.1), and the ORPA + B<sub>2</sub> approximation for the free energy, Eq. (2.2).

### B. Lennard-Jones fluid

The Lennard-Jones (LJ) fluid is the system in which the total potential energy is a sum of pair potentials of the form  $w_{\text{LJ}}(r) = 4\epsilon[(\sigma/r)^{12} - (\sigma/r)^6]$ . Here,  $\epsilon$  and  $\sigma$  are constants with units of energy and length, respectively.

Our analysis of this fluid begins with the separation of the potential into a reference part  $u_0(r)$  and a perturbation  $u(r)$ . An intelligent separation must satisfy two requirements. First,  $u_0(r)$  must be a harsh repulsive interaction.<sup>11</sup> This permits us to relate, as described below, the properties of the system with interactions  $u_0(r) + u(r)$  to the fluid with interactions  $u_d(r) + u(r)$ . The latter is the type of system that can be treated with the OCT as outlined in Sec. IIA.

The second requirement is that the high-density structure of the total system must be very close to that of the reference system. If this condition is satisfied, then  $\rho[g(r) - g_0(r)]$  is small, where  $g_0(r)$  is the reference system radial distribution function. This difference, of course, is of order  $\rho c(r)$  [see Eq. (2.1)], and  $\rho c(r)$  must be small for the OCT to be accurate. In other words, the OCT is a theory which calculates the effect of the perturbation on the structure of the fluid. If this effect (times the density) is small, the OCT is accurate.

A separation of the LJ potential which satisfies these two requirements is the one in which  $u_0(r)$  contains all the repulsive forces and none of the attractions, and  $u(r)$  contains all of the attractions. Mathematically the separation is

$$\begin{aligned} u_0(r) &= \epsilon + w_{\text{LJ}}(r), & r \leq r_0 \\ &= 0, & r > r_0 \end{aligned} \quad (2.3a)$$

and

$$\begin{aligned} u(r) &= -\epsilon, & r \leq r_0 \\ &= w_{\text{LJ}}(r), & r > r_0, \end{aligned} \quad (2.3b)$$

where  $r_0 = 2^{1/6}\sigma$ . The reference potential is indeed a harsh repulsion, and, as described in Sec. I, the high-density structure of the reference fluid is very close to that of the high-density LJ fluid.<sup>3,4</sup>

Since the reference interaction is not a hard-core repulsion, it is convenient to introduce a *trial* system for which the pair potential is  $w_T(r) = u_d(r) + u(r)$ . The OCT is used to predict the properties of the *trial* fluid. Once these are known, the properties of the LJ fluid are straightforwardly obtained through the application of a type of cluster expansion<sup>12</sup> (which is called the "blip function" expansion). The formulas needed to find the LJ properties from those of the *trial* system are given in Eqs. (11)–(14) of Ref. 4.

The optimized renormalized potential for the LJ *trial* system is graphed for three representative states in Fig. 1.

### C. Consistency of the theory

It is possible to unambiguously test the accuracy of the OCT on the LJ fluid because "exact" molecular dynamics and Monte Carlo calculations have been made on this system. However, the OCT is a general theory which is applicable to a wide variety of atomic liquids, liquid mixtures, and molecular liquids. As a result, one hopes that the theory will be applied to numerous systems which are of experimental interest but have not been investigated with computer simulations. Thus, it is important to be able to assess the accuracy of the OCT in the absence of exact nu-

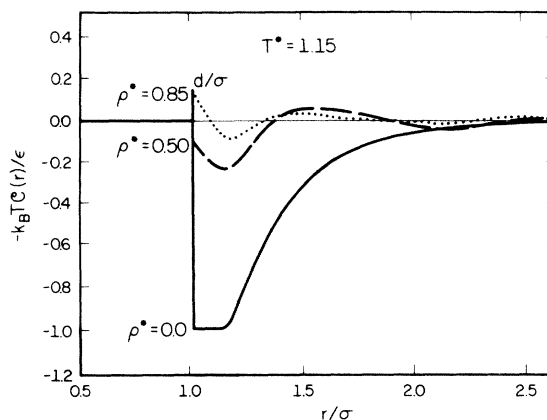


FIG. 1. Optimized renormalized potential for the *trial* system of the Lennard-Jones fluid at three representative thermodynamic states. For all three,  $k_B T/\epsilon = 1.15$ ; the densities are  $\rho\sigma^3 = 0.0$ ,  $\rho\sigma^3 = 0.50$ , and  $\rho\sigma^3 = 0.85$ .

merical results.

One satisfactory method for determining the accuracy is to estimate the relative size of the corrections to Eqs. (2.1) and (2.2). Since these corrections have been described explicitly in Ref. 6, this procedure is certainly a practical one. A detailed analysis of the order of magnitude of the corrections is given in Secs. V and VI of Ref. 6. In general, if the parameter  $\lambda$ , defined in Sec. IIA, is small, one knows that Eqs. (2.1) and (2.2) are accurate. If it is not small, one must either calculate higher-order terms in the optimized cluster expansions or devise a new separation of the intermolecular potential which satisfies the requirement discussed above that the high-density structure of the reference fluid is close to that of the total system (or, equivalently, find a separation that makes  $\lambda$  small).

Another method for testing the accuracy of the OCT is one that is usually used on theories for which it is not practical to evaluate corrections. This procedure calculates the equation of state from two (or more) different routes to the thermodynamics. The comparison of the results obtained from the different routes is regarded as a test of the internal consistency and thus the accuracy of the theory. We have applied this kind of test to the OCT for the LJ fluid. Let  $p_F$  denote the pressure obtained by differentiating the ORPA +  $B_2$  approximation for the free energy. Let  $p_v$  denote the pressure obtained from applying the virial theorem to the EXP approximation for  $g(r)$ . Then the following results are representative of what is found throughout the density-temperature plane:

$$\left. \begin{array}{l} \frac{p_F}{k_B T \rho} = 0.17 \\ \frac{p_v}{k_B T \rho} = 0.18 \end{array} \right\} \text{for } \rho \sigma^3 = 0.56 \text{ and } \frac{k_B T}{\epsilon} = 1.25,$$

and

$$\left. \begin{array}{l} \frac{p_F}{k_B T \rho} = 1.52 \\ \frac{p_v}{k_B T \rho} = 1.54 \end{array} \right\} \text{for } \rho \sigma^3 = 0.76 \text{ and } \frac{k_B T}{\epsilon} = 1.25.$$

The agreement between  $p_F$  and  $p_v$  is excellent. It is possible to attribute the entire difference between them to the uncertainty in our knowledge of the hard-sphere equation of state and of  $g_d(r)$ .<sup>13</sup> Both of these quantities are needed as input for our calculations.

The same consistency test can be applied to the high-temperature approximation<sup>3</sup> (HTA) which

completely neglects the effect of the attractive forces on the structure. At high densities,  $g_0(r)$  is indeed very close to  $g(r)$ . However, the approximation  $g(r) \approx g_0(r)$  is not accurate to several significant figures. But this kind of accuracy is required if the virial theorem pressures are to agree closely with those obtained by differentiating the free energy. Indeed, at the representative state  $\rho \sigma^3 = 0.80$  and  $k_B T / \epsilon = 1.35$ , the virial theorem applied to  $g(r) \approx g_0(r)$  gives  $p / k_B T \rho = 3.10$ , while differentiation of the free energy in the HTA gives  $p / k_B T \rho = 2.40$ . (Computer simulations<sup>14</sup> give 2.42.) Thus, the HTA, which is the zero-order theory in the optimized cluster expansions, is not a consistent theory in the sense that two independent routes to the thermodynamics give the same results. This should be expected for a zero-order theory. The first natural corrections to the HTA are Eqs. (2.1) and (2.2). It is seen that these equations do satisfy the consistency test to an excellent approximation.

### III. RESULTS

We now discuss the predictions of the OCT when it is applied to the LJ fluid for thermodynamic states in the neighborhood of the liquid-gas phase transition. Our results are expressed in terms of reduced variables for the temperature, density, and pressure; these are  $T^* = k_B T / \epsilon$ ,  $\rho^* = \rho \sigma^3$ , and  $p^* = p \sigma^3 / \epsilon$ , respectively.

In Sec. IIIA, thermodynamic properties are considered. In Sec. IIIB, the equilibrium pair correlation functions are discussed.

#### A. Thermodynamic properties

We have used Eq. (2.2) to calculate the Helmholtz free energy. By numerical differentiations, other thermodynamic properties were obtained.

For a few representative states, the OCT results are compared in Table I with those obtained from computer simulations.<sup>14</sup> The agreement is

TABLE I. Comparison of the results obtained from the optimized cluster theory (OCT) and Monte Carlo computer experiments (MC) for the Lennard-Jones fluid (Ref. 14).  $T^*$  and  $\rho^*$  denote the reduced temperature and density, respectively.  $\Delta A$  is the excess (with respect to the ideal gas) Helmholtz free energy;  $p$  is the pressure;  $\Delta E$  is the excess internal energy.

$T^*$	$\rho^*$	$-\Delta A / N k_B T$		$p / k_B T \rho$		$-\Delta E / N \epsilon$	
		MC	OCT	MC	OCT	MC	OCT
1.15	0.65	1.84	1.85	0.31	0.22	4.45	4.47
1.15	0.75	1.89	1.91	1.17	1.10	5.13	5.13
1.15	0.85	1.78	1.80	2.86	2.84	5.67	5.69
1.35	0.10	0.29	0.30	0.72	0.72	0.78	0.78
1.35	0.20	0.56	0.56	0.50	0.51	1.51	1.50

excellent. (Note that the uncertainty in the determination of  $p/k_B T \rho$  from computer experiments is  $\pm 0.05$  at liquid densities.)

We have found that at high densities ( $\rho^* \geq 0.65$ ), the ORPA +  $B_2$  free energy [Eq. (2.2)] is virtually indistinguishable from the optimized-random-phase approximation (ORPA) free energy discussed in Ref. 4. The reason for the agreement is that the difference between these two approximations is second order in the renormalized potential, and the renormalized potential is very small at high densities. Extensive comparison between the ORPA and computer simulations can be found in Ref. 4. It is seen there that at high densities, the ORPA (and thus the OCT) predictions agree with those of the computer experiments within the possible error of the latter.

With the free energy and pressure determined from the OCT, we have calculated the liquid-gas coexistence curve from a Maxwell construction. The results obtained are given in Table II and Fig. 2. Since the OCT is exact at very low densities<sup>6</sup> and nearly exact at very high densities,<sup>7</sup> the low-temperature portions of the coexistence curve must represent accurately the exact phase diagram of the LJ fluid. At higher temperatures, however, it is not obvious that the theory will remain precise.

Computer experiments have not been used to

TABLE II. Coexisting gas and liquid densities and the corresponding pressure of a Lennard-Jones fluid at various temperatures as calculated using the optimized cluster theory.

$T^*$	$\rho_g^{*a}$	$\rho_l^{*a}$	$p^{*a}$
1.345	0.309	0.384	0.146
1.340	0.282	0.404	0.143
1.335	0.264	0.419	0.140
1.330	0.249	0.432	0.137
1.325	0.236	0.443	0.134
1.320	0.224	0.452	0.131
1.315	0.214	0.461	0.129
1.310	0.204	0.469	0.126
1.305	0.196	0.477	0.123
1.300	0.188	0.484	0.121
1.295	0.180	0.491	0.118
1.290	0.174	0.497	0.115
1.250	0.131	0.541	0.096
1.200	0.096	0.584	0.076
1.150	0.072	0.621	0.059
1.100	0.053	0.653	0.045
1.050	0.039	0.682	0.034
0.950	0.020	0.734	0.017
0.850	0.009	0.781	0.007

<sup>a</sup> There are uncertainties in the third decimal place owing to the uncertainties in the hard-sphere equation of state used to calculate the OCT pressure (see Ref. 13).

make extensive studies of the liquid-gas phase diagram. The only accurate study at a temperature significantly higher than the triple point temperature (which is  $T^* = 0.70$ ) is the calculation of Hansen and Verlet for the isotherm  $T^* = 1.15$ .<sup>14</sup> At this temperature, they find that the densities of the coexisting gas and liquid are  $\rho_g^* = 0.073$  and  $\rho_l^* = 0.606$ , respectively, and the pressure of the coexisting phases is  $p^* = 0.0597$ . These numbers agree exceptionally well with the entries in Table II. Thus, we conclude that the coexistence curve predicted by the OCT is quantitatively accurate for  $T^* \leq 1.15$ .

For reduced temperatures greater than 1.15, critical-point singularities begin to become important in forming the nature of the coexistence curve. Thus, even if computer simulations were done to predict the phase diagram for  $T^* > 1.15$ , they would not provide a test for the theory. The computer experiments are performed on small systems. As a result, they cannot duplicate the behavior of a macroscopic fluid with long-ranged correlations. To study the prediction of the OCT in the critical region, we have tried to compare our calculations with experiments on real liquid argon. The principal difficulty with this approach is that the LJ potential does not represent quantitatively the interactions between argon atoms.<sup>15</sup> However, the comparison should provide a qualitative test of the OCT.

From the juxtaposition of the theoretical coexistence curve and the curve for argon,<sup>16</sup> we find that the "best" fit is obtained with the LJ param-

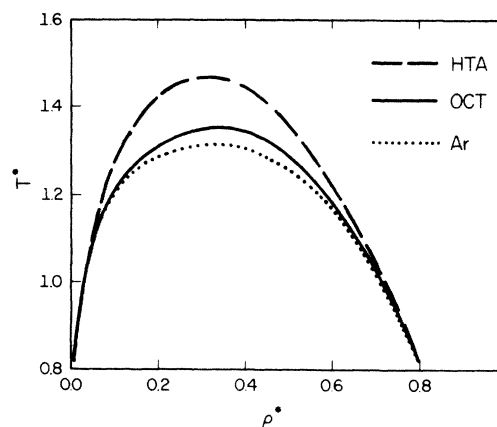


FIG. 2. Liquid-gas coexistence curve of the Lennard-Jones fluid in the temperature-density plane. The solid curve is obtained from the optimized cluster theory [Eq. (2.2)], the dashed curve from the high-temperature approximation (Ref. 3), and the dotted curve from the experimental results for argon (Ref. 16) assuming that argon is a Lennard-Jones fluid with the parameters equal to those described in the text.

eters given by  $\sigma = 3.401 \text{ \AA}$  and  $\epsilon/k_B = 115.8 \text{ }^\circ\text{K}$ . These values are similar to (but not the same as) those found by Michels *et al.*<sup>17</sup> from fits of the low-density properties of argon; and they are also similar to the parameters that Verlet and Weis<sup>18</sup> found from considering the high-density properties of argon. The criterion we used to find the "best"  $\epsilon$  and  $\sigma$  was based on the conclusion, stated above, that for  $T^* \leq 1.15$ , the OCT provides a quantitative description of the LJ coexistence curve. Therefore, we determined the LJ parameters for which the theoretical phase diagram in that temperature region agrees as closely as possible with the argon phase diagram.

With the above stated values for  $\sigma$  and  $\epsilon$ , the experimental argon coexistence curve is shown in Fig. 2. Very close to the critical point the OCT disagrees with experiment. The disagreement is large enough that it must be due to errors in the OCT and not to inadequacies in the LJ potential as a model for interactions in liquid argon. With our values of  $\sigma$  and  $\epsilon$ , the experimental critical point is  $T_c^*(\text{expt}) = 1.303$ ,  $\rho_c^*(\text{expt}) = 0.318$ , and  $p_c^*(\text{expt}) = 0.121$ . The OCT predicts  $T_c^* = 1.348$ ,  $\rho_c^* = 0.349$ , and  $p_c^* = 0.148$ .

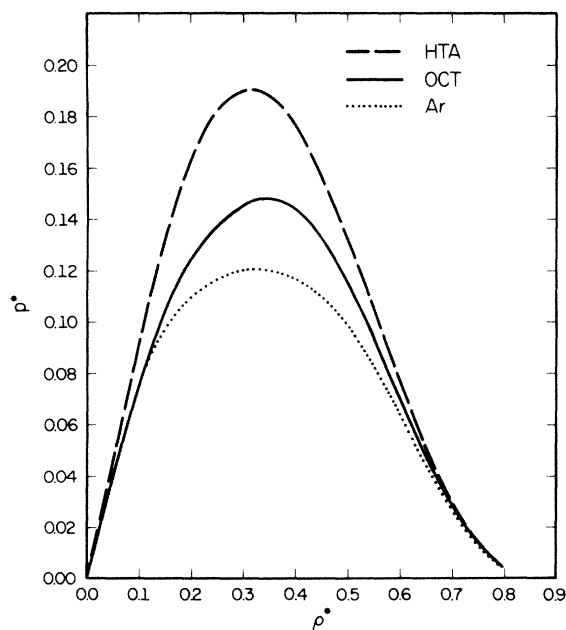


FIG. 3. Liquid-gas coexistence curve of the Lennard-Jones fluid in the pressure-density plane. The solid curve is obtained from the optimized cluster theory [Eq. (2.2)], the dashed curve from the high-temperature approximation (Ref. 3), and the dotted curve from the experimental results for argon (Ref. 16) assuming that argon is a Lennard-Jones fluid with the parameters equal to those described in the text.

Incidentally, on the basis of PY II equation calculations, Verlet and co-workers have estimated the critical constants to be  $T_c^*$  (Verlet) =  $1.36 \pm 0.04$ ,  $\rho_c^*$  (Verlet) =  $0.36 \pm 0.03$ , and  $p_c^*$  (Verlet) =  $0.15 \pm 0.015$ .<sup>14</sup>

The coexistence curve obtained from the HTA is also shown in Fig. 2. This simple perturbation theory does not describe the phase diagram accurately because the HTA neglects entirely the effects of the attractive forces on the fluid structure. It is seen that the OCT makes an important improvement on the HTA.

The representation of the coexistence curves in the pressure-density plane is shown in Fig. 3.

The pressure calculated from the OCT at several thermodynamic states near the coexistence curve are tabulated in Table III. Also given are the experimental values for argon.<sup>16</sup> The differences between experiment and theory are sufficiently small that they can be attributed entirely to the inaccuracies of the LJ potential model for the interactions in liquid argon.

It is well known that an analytic free energy supplemented with the Maxwell construction yields a "classical" theory of phase transitions.<sup>19</sup> Thus, the OCT is a classical theory, and it should be no surprise that an examination of our calculations very close to the critical point yields the following classical values for the critical exponents:  $\beta = \frac{1}{2}$ ,  $\gamma = \gamma' = 1$ ,  $\delta = 3$ ,  $\alpha = \alpha' = 0$ . Here, the Greek letters stand for the usual critical indices defined in Ref. 19. For example, the exponent  $\beta$  describes the curvature of the liquid-gas phase diagram asymptotically close to the critical point; i.e.,

TABLE III. Comparison of pressures calculated from the optimized cluster theory (OCT) with the corresponding experimental argon values of Ref. 16 (expt). It is assumed here that argon is a Lennard-Jones fluid with the Lennard-Jones parameters discussed in the text.

$T^*$	$\rho^*$	$p^*$	
		OCT	expt
1.269	0.662	0.55	0.55
1.269	0.757	1.51	1.50
1.356	0.166	0.13	0.12
1.356	0.313	0.15	0.15
1.356	0.433	0.16	0.17
1.356	0.477	0.18	0.20
1.356	0.571	0.34	0.35
1.356	0.674	0.88	0.87
1.425	0.351	0.20	0.20
1.425	0.447	0.24	0.25
1.425	0.546	0.39	0.40
1.425	0.603	0.60	0.60
1.425	0.716	1.51	1.50
1.425	0.780	2.51	2.49

$$\beta = \lim_{T^* \rightarrow T_c^*} [\ln(\rho_l^* - \rho_g^*) / \ln(T_c^* - T^*)].$$

The plot of  $\ln(\rho_l^* - \rho_g^*)$  vs  $\ln(T_c^* - T^*)$  that is obtained from the OCT is shown in Fig. 4.

While the OCT is a classical theory, it can yield quantitative results provided one is not too close to the critical point. It is seen that for temperatures 20% away from  $T_c^*$ , the plot in Fig. 4 can be accurately represented by a line with a slope of approximately  $\frac{1}{3}$ . Since the experimental value for  $\beta$  is near  $\frac{1}{3}$ , Fig. 4 suggests that the OCT predictions outside of the critical region can be used to extrapolate to the critical point.

We assume that for states significantly far away from the critical point, the coexistence curve can be represented by the following equation:

$$\rho_l^* - \rho_g^* = A [T_c^*(\text{ext}) - T^*]^{\beta(\text{ext})}. \quad (3.1)$$

Here, "ext" is used to denote "extrapolated value." It is emphasized that  $\beta(\text{ext})$  is rigorously not the critical exponent  $\beta$  because  $\beta$  is defined in the limit asymptotically close to the critical point. The constants  $A$ ,  $T_c^*(\text{ext})$ , and  $\beta(\text{ext})$  are determined by fitting Eq. (3.1) to the coexistence curve at three temperatures in the region for which the OCT is accurate ( $T^* \leq 1.15$ ). Depending on which three temperatures are used, slightly different values for the constants are obtained. However, the numbers are stable enough that we can make

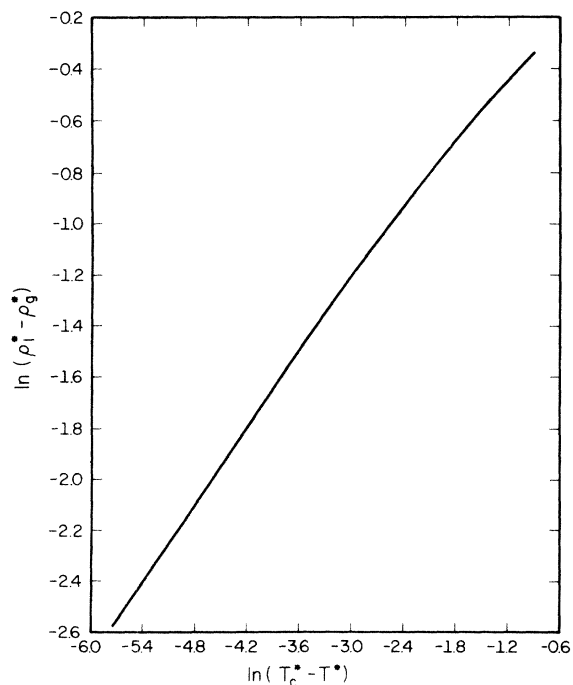


FIG. 4. Optimized cluster theory coexistence curve:  $\ln(\rho_l^* - \rho_g^*)$  vs  $\ln(T_c^* - T^*)$ .

fairly specific predictions. These are:  $\beta(\text{ext}) = 0.33 \pm 0.03$  and  $T_c^*(\text{ext}) = 1.31 \pm 0.01$ . The value for the extrapolated critical temperature  $T_c^*(\text{ext})$  compares favorably with the experimental value (stated above) of 1.303. Further,  $\beta(\text{ext})$  compares well with the experimental value of  $\beta(\text{expt}) \approx 0.36$ .<sup>20</sup>

We have also used the extrapolation procedure to study the critical exponent  $\gamma$  which describes the divergence of the isothermal compressibility,  $K_T$ , for temperatures above  $T_c^*$  and for densities on the critical isochore. The extrapolation formula we used is

$$K_T = B [T^* - T_c^*(\text{ext})]^{-\gamma(\text{ext})}$$

for  $T^* \geq T_c^*(\text{ext})$  and  $\rho^* = \rho_c^*(\text{ext})$ . To determine the constants, the OCT values for  $K_T$  were found for  $T^* \geq 1.45$ . The procedure gives  $\gamma(\text{ext}) = 1.27 \pm 0.07$ . The value agrees well with the experimentally measured critical exponent  $\gamma(\text{expt}) \approx 1.2$ .<sup>19, 21</sup>

For completeness, the OCT prediction of the heat capacity  $C_V$  along the critical isochore is shown in Fig. 5.

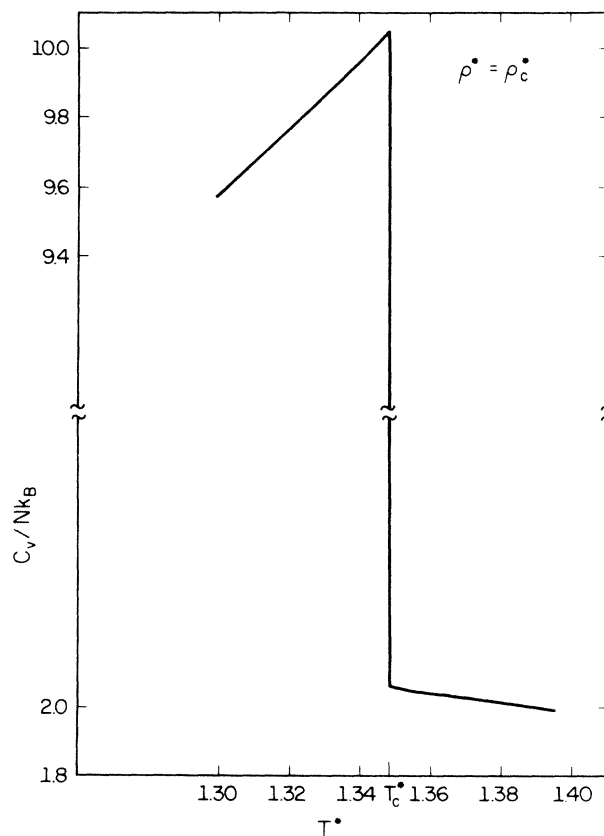


FIG. 5. Constant-volume heat capacity  $C_V$  calculated from the optimized cluster theory along the theoretical critical isochore  $\rho_c^* = 0.349$ .

## B. Structural properties

We now discuss the results obtained from the EXP approximation for the pair correlation function [Eq. (2.1)].

Two representative calculations have already been presented in Ref. 7. These were at the thermodynamic states  $T^*=1.36$ ,  $\rho^*=0.50$  and  $T^*=0.88$ ,  $\rho^*=0.85$ . In both cases, it was shown that the  $g(r)$  calculated from the EXP approximation agrees with the molecular dynamics  $g(r)$  within the possible error of the computer experiment.

In Fig. 6, we show the pair correlation function at the state which is the critical point obtained from the OCT free energy. An integration over  $g(r) - 1$  shows that the OCT  $g(r)$  approaches the asymptotic value of unity in a *finite* range. Thus, an important physical feature of the critical point (long-ranged correlations) is not contained in the OCT. Further, because the range is finite, the compressibility predicted from the EXP approximation for  $g(r)$  is finite. The ORPA +  $B_2$  free energy, of course, predicts an infinite compressibility. Thus, the OCT is inconsistent at the critical point. This should be expected since we have already pointed out that the OCT provides a classical (and thus incorrect) theory of the critical point.

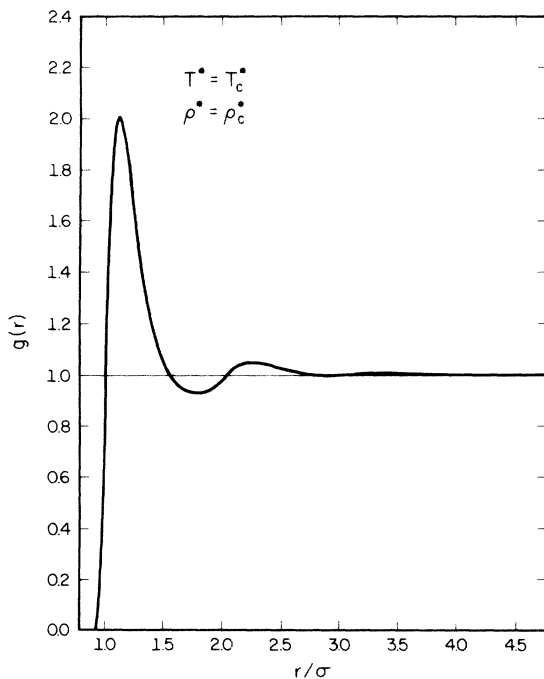


FIG. 6. Radial distribution function calculated from the optimized cluster theory at the theoretical critical point ( $\rho_c^*=0.349$  and  $T_c^*=1.348$ ).

In Fig. 7, we show the EXP approximation for  $g(r)$  at three different densities on the  $T^*=1.249$  isotherm. The states are sufficiently far from the critical point that we believe the curves are quantitative representations of the exact  $g(r)$ . Our results shown in Fig. 7 support the conjecture of Fisher and Widom<sup>22</sup> that there is a boundary in the temperature-density plane such that the asymptotic decay of the pair correlation function is monotonic on the low-density side and oscillatory on the high-density side (see Fig. 7 of Ref. 22). The same remarks apply to Fig. 8, which shows  $g(r)$  calculated from the EXP approximation for a low- and a high-density state on the isotherm  $T^*=1.351$ .

The structure factor,  $S(k)$ , is defined as

$$S(k) = 1 + \rho \int [g(r) - 1] e^{-i\vec{k}\cdot\vec{r}} d\vec{r}.$$

By Fourier transforming the pair correlation function in the EXP approximation, we have calculated  $S(k)$ . In Fig. 9 we show  $S(k)$  so obtained on the OCT critical isochore,  $\rho^* = \rho_c^*$ , at the temperatures  $T^* = T_c^*$ ,  $T^* = 1.45$ , and  $T^* = 1.55$ . The fact that  $S(0)$  is not infinite at the critical point was discussed above and it is an indication of the inconsistencies of the OCT near the critical point. It is significant that the EXP approxi-

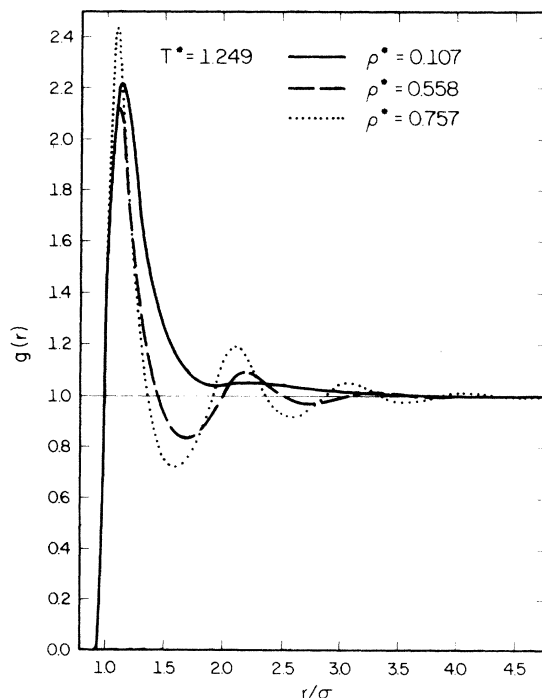


FIG. 7. Radial distribution function for states on the  $T^*=1.249$  isotherm. The three densities are  $\rho^*=0.107$ ,  $\rho^*=0.558$ , and  $\rho^*=0.757$ .



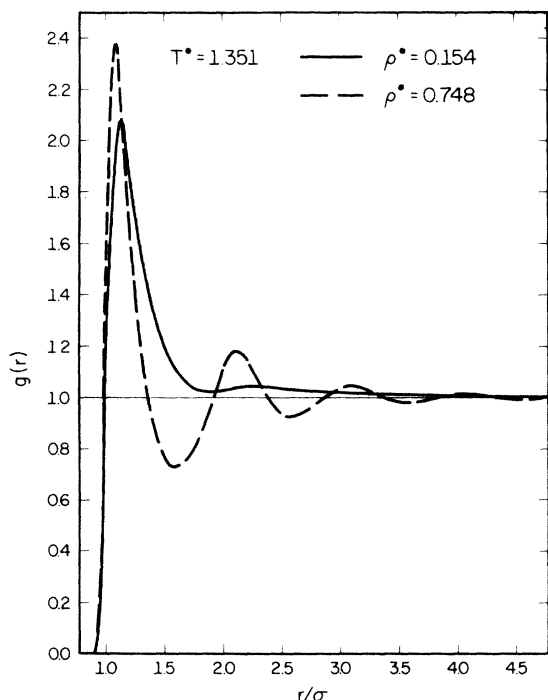


FIG. 8. Radial distribution function for states on the  $T^* = 1.351$  isotherm. The two densities are  $\rho^* = 0.154$  and  $\rho^* = 0.748$ .

mation predicts  $S(0) > 2$  at the critical point. This is an order of magnitude greater than the HTA (unperturbed) value. Thus, the OCT predicts a large effect due to the attractive forces. As discussed in Sec. II, the prediction of a large effect on the structure by the OCT is a signal that Eqs. (2.1) and (2.2) may no longer be quantitatively precise.

The two higher-temperature states shown in Fig. 9 are far enough removed from the critical point that the structure factors shown for those states should be quantitatively accurate. Note that except for small  $k$ , the structure factors change very little as the temperature is changed.

#### IV. DISCUSSION

In this paper we have presented several new calculations using the optimized cluster theory. We believe the most significant of these are the calculation of the coexistence curve and the extrapolation procedures used to determine the critical exponents.

To our knowledge, the OCT coexistence curve presented herein represents the most accurate microscopic calculation of a coexistence curve for a fluid with a realistic Hamiltonian. Very close to the critical point, the OCT fails to be

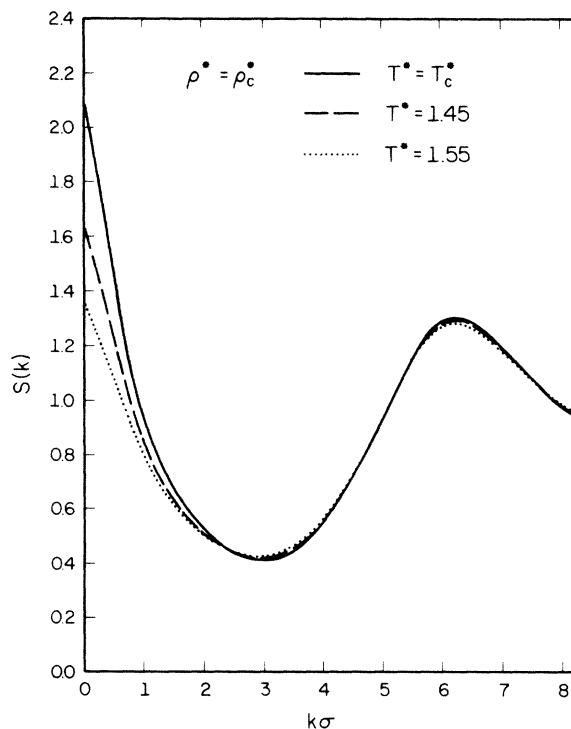


FIG. 9. Structure factor  $S(k)$  of the Lennard-Jones fluid calculated from the optimized cluster theory. The three thermodynamic states lie on the theoretical critical isochore ( $\rho_c^* = 0.349$ ). The temperatures are  $T^* = T_c^* = 1.348$ ,  $T^* = 1.45$ , and  $T^* = 1.55$ .

accurate. The reason is that the range of the renormalized potential becomes relatively large in the critical region [recall that  $S(0) > 2$  at the OCT critical point]. As a result, the expansion parameter in the optimized cluster expansions is not small in that region. Nevertheless, from the computations discussed in this paper, we are confident that the OCT is quantitatively precise for thermodynamic states which have temperatures that differ from  $T_c^*$  (expt) by at least 10% and/or have densities that differ from  $\rho_c^*$  (expt) by 0.15 or more.

We have shown that the precision of the OCT outside of the critical region can be used to extrapolate towards the critical point. The extrapolation procedures introduced in this paper are not rigorous calculations of critical exponents. However, they unambiguously predict nonclassical values for the critical exponents and the predicted values are in good agreement with experiment.

#### ACKNOWLEDGMENT

We are grateful to Michael Wortis for many informative discussions and helpful suggestions.

- \*Research supported by the National Science Foundation, and the donors of the Petroleum Research Fund administered by the American Chemical Society.
- †Alfred P. Sloan Foundation Research Fellow.
- <sup>1</sup>For a recent review, see J. A. Barker and D. Henderson, *Annu. Rev. Phys. Chem.* **23**, 439 (1972).
- <sup>2</sup>D. Chandler and J. D. Weeks, *Phys. Rev. Lett.* **25**, 149 (1970).
- <sup>3</sup>J. D. Weeks, D. Chandler, and H. C. Andersen, *J. Chem. Phys.* **54**, 5237 (1971); *J. Chem. Phys.* **55**, 5421 (1971).
- <sup>4</sup>H. C. Andersen, D. Chandler, and J. D. Weeks, *J. Chem. Phys.* **56**, 3812 (1972).
- <sup>5</sup>Strictly speaking, "attractive interactions" should be replaced by "slowly varying attractions and repulsions." For example, the oscillatory part of the effective pair potential in liquid metals (which contains repulsions as well as attractions) does not contribute very much to the structure of those systems. However, the quickly varying repulsive core does. See D. Schiff, *Phys. Rev.* **186**, 151 (1969).
- <sup>6</sup>H. C. Andersen and D. Chandler, *J. Chem. Phys.* **57**, 1918 (1972).
- <sup>7</sup>H. C. Andersen, D. Chandler, and J. D. Weeks, *J. Chem. Phys.* **57**, 2626 (1972).
- <sup>8</sup>H. C. Andersen and D. Chandler (unpublished).
- <sup>9</sup>L. Verlet and J.-J. Weis, *Phys. Rev. A* **5**, 939 (1972).
- <sup>10</sup>N. F. Carnahan and K. E. Starling, *J. Chem. Phys.* **51**, 635 (1969).
- <sup>11</sup>In saying that  $u_0(r)$  is a "harsh repulsion" we mean that the Boltzmann factor for  $u_0(r)$ ,  $\exp[-u_0(r)/k_B T]$ , closely resembles the Boltzmann factor for the hard-sphere interactions (which is a step function rising from 0 to 1 at a distance corresponding to the hard-sphere diameter  $d$ ). In particular,  $\exp[-u_0(r)/k_B T]$  must be zero for small  $r$ , unity for large  $r$ , and it must rise from essentially zero to essentially unity over a range of  $r$  values which is small compared with the  $r$  at which it has the value of  $\frac{1}{2}$ .
- <sup>12</sup>H. C. Andersen, J. D. Weeks, and D. Chandler, *Phys. Rev. A* **4**, 1597 (1971).
- <sup>13</sup>We use the Verlet-Weis formula for  $g_d(r)$  (Ref. 9) and the Carnahan-Starling formula for the hard-sphere equation of state (Ref. 10). At liquid densities, the errors in the Verlet-Weis formula can be as large as 0.03. Similarly, the Carnahan-Starling formula for  $p_d/k_B T\rho$  might have errors of that order of magnitude at high densities. See further remarks concerning these matters in footnote 18 of Ref. 12.
- <sup>14</sup>Thermodynamic properties obtained by molecular dynamics computations on the LJ fluid are tabulated by L. Verlet, *Phys. Rev.* **159**, 98 (1967). Monte Carlo calculations are reported by D. Levesque and L. Verlet, *Phys. Rev.* **182**, 307 (1969), and by J.-P. Hansen and L. Verlet, *Phys. Rev.* **184**, 151 (1969). A convenient summary of much of the available computer data on the LJ fluid is found in Ref. 9. The critical constants usually referred to by Verlet and coworkers are obtained from the solution of the PY II equation: L. Verlet and D. Levesque, *Physica (Utr.)* **36**, 254 (1967).
- <sup>15</sup>J. A. Barker, R. A. Fisher, and R. O. Watts, *Mol. Phys.* **21**, 657 (1971).
- <sup>16</sup>A. L. Gosman, R. D. McCarty, and J. G. Hust, *Thermodynamic Properties of Argon From the Triple Point to 300°K at Pressures to 1000 Atmospheres* (U. S. Dept. of Commerce, N. B. S., Boulder, Colorado, 1969).
- <sup>17</sup>A. Michels, H. Wijker, and H. K. Wijker, *Physica (Utr.)* **15**, 627 (1949).
- <sup>18</sup>L. Verlet and J.-J. Weis, *Mol. Phys.* **24**, 1013 (1972).
- <sup>19</sup>M. E. Fisher, *Rep. Prog. Phys.* **30**, 615 (1967).
- <sup>20</sup>J. M. H. Levelt Sengers, *Ind. Eng. Chem. Fundam.* **9**, 470 (1970).
- <sup>21</sup>P. Heller, *Rep. Prog. Phys.* **30**, 731 (1967).
- <sup>22</sup>M. E. Fisher and B. Widom, *J. Chem. Phys.* **50**, 3756 (1969).